Entropy Controlled Phase Shift Migration with De-Noising Algorithm for RADAR Body Area Focussing Imaging

Hui Zhang
Technische Universität Dresden
01062,Dresden,Germany
hui.zhang@mailbox.tu-dresden.de

Yun Lu
Technische Universität Dresden
01062,Dresden,Germany
yun.lu1@tu-dresden.de

Dirk Plettemeier
Technische Universität Dresden
01062,Dresden,Germany
dirk.plettemeier@tu-dresden.de

ABSTRACT

In this paper we propose an entropy-based phase shift migration algorithm (EBPSM) combined with a preprocessing de-noising step. We apply these algorithms to human body radar-imaging. As measure for the evaluation of the algorithms performance and for comparison with different approaches we chose the detection rate and the false alarm rate. For measurement and simulated data we can demonstrate the benefits of the EBPSM which has a higher detection rate while maintaining a lower false alarm rate in comparison to previous algorithms. In addition the EBPSM exhibits good 3D focussing properties yielding proper imaging results.

Categories and Subject Descriptors

F.2 [**ANALYSIS OF ALGORITHMS AND PROBLEM COMPLEXITY**]: General

Keywords

Human Body RADAR-Imaging, De-Noising, Compressive Sensing, Human Spine

1. INTRODUCTION

In these decades, the radar detecting techniques are applied on human body area imaging. Radar system transmits the EM wave towards the human body. Parts of the EM wave will be reflected from the interfaces of two adjacent different materials. Based on the phase delays of the reflected EM waves, the shapes of interfaces could be reconstructed so that the inner structure of the human body can be detected. For human body area radar imaging, the main challenging things are inhomogeneous material scenario and large attenuation for high frequency signal. Because human body is an inhomogeneous material, the conventional radar imaging technique becomes feeble. Due to the high attenuation for high frequency, the bandwidth of the employed signal by radar system is thin and the SNR of the received reflection signal is low. Therefore, the resolution of the obtained radar images by conventional radar imaging technique is bad. For solving the inhomogeneous material radar imaging problem, the EBPSM is introduced, analysed and applied. EBPSM can be mainly divided into two steps. First step is applying the phase shift migration (PSM) radar imaging algorithm on the received data to obtain the radar images, the second step is as to apply image entropy analyse algorithm, which can help us find the suitable parameter in the phase shift migration algorithm. PSM originates from the solution of the homogeneous EM wave equation. It obtains the EM field distribution through the EM field extrapolation in wave-number frequency domain. The suitable extrapolation factor is determined by analysing obtained images entropy. According to the scattering EM field distribution, the position and shape of objects or interfaces can be finally determined. In practical radar imaging measurement, the noise will affect the obtained radar images. In order to achieve better and clearer radar images, a specified de-noising algorithm will be applied before EBPSM as a preprocessing step.

BODYNETS 2014, September 29-October 01, London, Great Britain

DOI 10.4108/icst.bodynets.2014.257127

2. THE PRINCIPLE OF EBPSM

EBPSM is a two step algorithm derived from phase migration. In the first section of this chapter we describe and analyse the basics of phase migration. In the second section we introduce the improvements of the EBPSM over standard phase migration. Finally, in the third section we describe and analyse the effect of noise on the proposed algorithm.

2.1 Phase shift migration algorithm

To simplify the analysing, let us consider the 2D radar imaging problem. The configuration schematic diagram of the radar imaging system is as figure 1. The radar is on the plane $z_0 = 0$ and moves from left side to right side along x-axis. During the moving, radar transmits the EM wave and receives the reflected signal from the illuminated surface, subsurface and buried objects. Symbol x is the coordinate in the radar aperture dimension(radar moving direction), symbol z is the coordinate in the range dimension. Since we discuss 2D radar subsurface imaging, the EM field distribution along y-axis is assumed to be constant. According to the EM wave equation, an EM field $U(x, y, \omega)$ can be described by the following scalar wave equation:

$$[\frac{\partial^2}{\partial x^2} + \frac{\partial^2}{\partial z^2} - \frac{\omega^2}{v_m^2}]U(x, z, \omega) = 0 \quad (1)$$

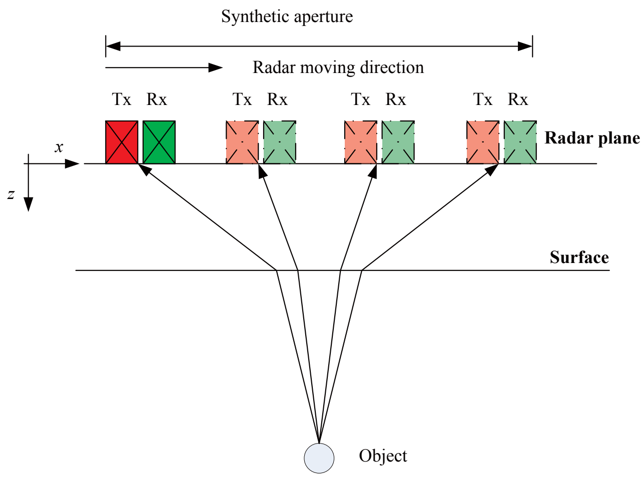

Figure 1: Ground penetrating radar system

where v_m is the electromagnetic wave propagation velocity in the material (medium). Equation is a multi variable second order partial differential equation (PDE).

The solution of the equation (1) in wave-number frequency domain can be expressed as[1][3]:

$$U(k_x, z, \omega) = U(k_x, 0, \omega) e^{-jz\sqrt{\frac{\omega^2}{v_m^2} - k_x^2}} \tag{2}$$

where $U(k_x, 0, \omega)$ is the scattering electromagnetic field in frequency wave number domain at plane $z = 0$, where is assigned as the radar plane. When EM wave propagates through inhomogeneous medium, the wave propagation velocity is inconstant. In this case, the solution can be expressed by recursive equation as:

$$U(k_x, z = (i+1)\Delta z, \omega) = U(k_x, z = i\Delta z, \omega) e^{-j\Delta z\sqrt{\frac{\omega^2}{v_m(i)^2} - k_x^2}} \tag{3}$$

The more detail about the solution deduction can be found in our reference [3]. $U(k_x, 0, \omega)$ can be obtained by applying Fourier transform, along x direction, on $u(x, z = 0, \omega)$, which is radar measurement data. The propagation velocity $v_m(i)$ is determined by the material permittivity on the position $z = i\Delta z$. By recursively extrapolating the scattering EM field in wave number-frequency domain along the z-axis, the distribution of the scattering field $U(k_x, z, \omega)$ can be reconstructed. Further, the electromagnetic field distribution $u(x, z, t)$ in time-space domain can be calculated by using inverse Fourier transform on $U(k_x, z, \omega)$ as equation (4)

$$u(x, z = z_1, t) = \frac{1}{4\pi^2} \int\int U(k_x, z = z_1, \omega) e^{jk_x x} e^{j\omega t} dk_x df \tag{4}$$

The scattering electromagnetic field $u(x, z, t)$ can be equivalently seen as the measured scattering EM field when the radar scanning on the plane z. Therefore $u(x, z, t = 0)$ is the radar received data at the time equal to zero on the position (x, z), which also means local the reflection intensity on the point (x, z). Therefore the reflectivity function can be determined as $\Gamma(x, z) = u(x, z, t = 0)$. According to reflectivity function $\Gamma(x, z)$, the focused radar image can be obtained.

2.2 EBPSM algorithm

As above description, the determination of the propagation velocity $v_m(i)$ in the phase migration factor is very important for the phase shift migration algorithm. However, the propagation velocity is decided by the material permittivity, which is unknown. In order to estimate the propagation velocity $v_m(i)$, image entropy calculation is applied. The detailed processing step is as following: Step 1. We assign the propagation velocity as light speed as $v_m = c$ for all inhomogeneous material layer. After phase shift migration processing, the layer structure in equivalent light speed mode is obtained. The light speed layer mode is described as reference [4]. Therefore, the interfaces positions $z_{c1}, z_{c2}, z_{c3}, ...$ in equivalent light speed mode are obtained. Step 2. Phase shift migration is applied again for imaging the first layer with different propagation velocity v_m. Obviously, the estimated interfaces position of the first layer is different when the given estimated propagation velocity v_m is different. It can be expressed as $z_{v1} = z_{c1}/c * v_m$. We defining I as the obtained radar images. The radar images for first layer with different estimated velocity, $I_1, I_2, ..., I_n, ..$ are obtained by phase shift migration algorithm. Step 3. The entropy of the first layer images $I_1, I_2, ..., I_n, ..$ are calculated. The given velocity corresponding to the image with minimum entropy is considered as the propagation velocity for the first layer v_{m1}. Meanwhile the image with minimum entropy is considered as the image for the first layer I_{l1}. Step 4. According to equation (2), the EM field on the first interface $u(x, z = z_{v1}, t = 0)$ is extrapolated with estimated first layer velocity v_{m1}. The first interface is seen as the equivalent radar scan plane. The measured data $U(x, z = 0, \omega)$ is uploaded by $u(x, z = z_{v1}, \omega)$. In this condition, the interfaces position in equivalent light speed mode are $z_{c2}, z_{c3}, ...$ Redoing the step 2 and step 3 results the focused image for second layer. Repeating the step 2, step 3 and step 4, the focused images for each layer are obtained. Finally the focused radar image for whole inhomogeneous material is achieved. The procedure steps of EBPSM and phase migration are as figure 2. The image is focused layer by layer through applying EBPSM.

2.3 Noise effect on EBPSM

In the practical measurement, the noise will affect the EBPSM imaging quality. The effect of noise on the EBPSM radar imaging, in 2-D radar measurement case, will be shortly discussed in this subsection. The radar received signal with noise can be expressed as:

$$\hat{U}(x, z = 0, \omega) = U(x, z = 0, \omega) + n(x, \omega) \tag{5}$$

After the EBPSM processing, the noise effect on position (x, z) is as:

$$\begin{aligned} N_{EBPSM} &= \iint n(k_x, \omega) e^{-j\Delta z\sqrt{\frac{\omega^2}{v_m(i)^2} - k_x^2}} e^{jk_x x} dx d\omega \\ &= \iiint n(x', \omega) e^{-j\Delta z\sqrt{\frac{\omega^2}{v_m^2} - k_x^2} + jk_x(x - x')} dk_x dx d\omega \end{aligned} \tag{6}$$

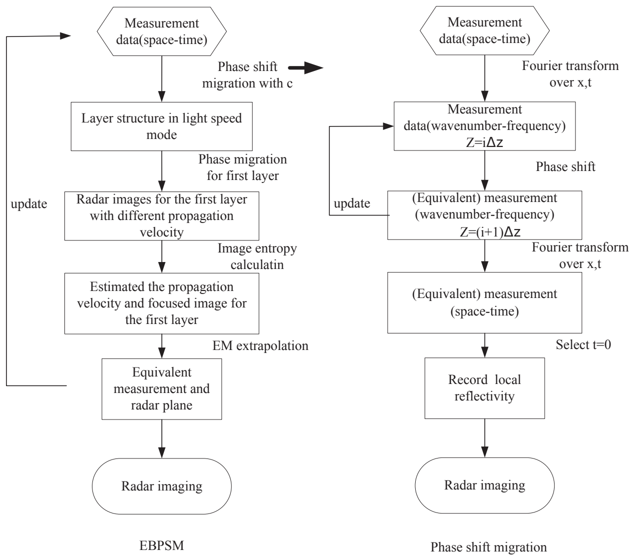

Figure 2: procedure steps of EBPSM and phase shift migration

Assigning $\Delta x = x - x'$ and $R = \sqrt{\Delta x^2 + \Delta z^2}$, the integration with respect to k_x in equation(6) is:

$$W(R,\omega) = \int e^{-j\Delta z\sqrt{\frac{\omega^2}{v_m^2} - k_x^2} + jk_x\Delta x} dk_x \tag{7}$$

According to the stationary phase theory, the equation (7) can be expressed as:

$$W(R,\omega) \approx \sqrt{\frac{4\pi}{v_m R}}\sqrt{j\omega}e^{j2\omega\frac{R}{v_m}} = w(R,\omega)e^{j2\omega\frac{R}{v_m}} \tag{8}$$

Where $w(R,\omega) = \sqrt{\frac{4\pi}{v_m R}}\sqrt{j\omega}$. Substituting equation (8) into equation(6) results

$$\begin{aligned} N_{EBPSM} &\approx \iint n(x,\omega)w(R,\omega)e^{j2\omega\frac{R}{v_m}} dx d\omega \\ &= \int (\int n(x,\omega)w(R,\omega)e^{j2\omega\frac{R}{v_m}} d\omega)dx \end{aligned} \tag{9}$$

The noise is assumed as a Gaussian white noise $\mathcal{N}(0,\sigma^2)$. The signal frequency bandwidth is B. According to equation (9), the mean output noise power on the position (x_0, z_0) is as :

$$\begin{aligned} P_{N_{EBPSM}} &= \iiiint < n(x,\omega)n^*(x',\omega') > w(R,\omega) \\ &\quad w^*(R',\omega')e^{j2\omega\frac{R-R'}{v_m}} dx d\omega dx' d\omega' \\ &\approx \iint \frac{N_0}{2}|w(R,\omega)|^2 dx d\omega \\ &\approx \frac{z_0 N_0(2f_c + B)B}{2v_m} \end{aligned} \tag{10}$$

Where f_c is the centre frequency, z_0 is the position of the target on range direction. Symbol <> denotes the expected value. According to equation (10), the noising effect on each pixel of the obtained image. It is necessary to reduce the noise effect on the quality of EBPSM imaging.

3. NOISE MITIGATED METHOD

As mentioned above, the quality of imaging is strongly depending on the stability of received signals, which is furthermore related with SNR in channel as well as the interference caused by e.g. multipath components. Therefore, a pre-processing to reduce both noise and interference is very important. According to the basic principle of stepped frequency radar, the received signal can be well approximated in Fourier domain, namely

$$y_M = F_s x + \epsilon_M, \tag{11}$$

where $y_M \in \mathbb{C}^{n\times 1}$, $F_s \in \mathbb{C}^{n\times d}$, $x \in \mathbb{C}^{d\times 1}$ and ϵ_M are received data in frequency domain, a wide subset of FFT matrix, desired vector in time domain (it is also related with channel impulse response) and the additive noise, respectively. In other words, x is assumed to be well sparsely spanned in F_s and more generally dominated by strong components, i.e. x is compressible in F_s. Thus, $de-noising$ can be conducted by solving following sparse decoder

$$\min \|F_s x - y_M\|_2^2 + \lambda \|x\|_p^p, \quad p \in [0,1] \tag{12}$$

The problem of (12) is based on the least squares method with an additional fixed regularization prior of the form $\mathbf{p}(x) \sim \exp\Big(-\|x\|_p^p\Big)$, with $p \in [0,1]$. Given this prior, maximum a posteriori (MAP) solutions can be given as

$$\begin{aligned} \hat{x} &= \arg\max_x \mathbf{p}(x|y_M) \\ &= \arg\min_x -\log\mathbf{p}(y_M|x) - \log\mathbf{p}(x). \end{aligned} \tag{13}$$

which yields the cost function in (12). Alternatively, instead of giving a fixed prior as in MAP the Bayesian methods learn the prior from the observed data y_M, where an approximate prior is given with γ_i, which control the variance of each weight x_i: $\mathbf{p}_\gamma(x)=\prod_i \mathcal{N}(x_i;0,\gamma_i)\varphi(\gamma_i)$, where $\varphi(\gamma_i)$ is a non-negative function and $\mathcal{N}(x)$ is the Gaussian distribution over x. The approximate posterior is then

$$\mathbf{p}_\gamma(x|y_M) = \frac{\mathbf{p}(y_M|x)\mathbf{p}_\gamma(x)}{\int \mathbf{p}(y_M|x)\mathbf{p}_\gamma(x)dx} = \mathcal{N}(x;\mu_x,\Sigma_x) \tag{14}$$

with

$$\begin{aligned} \Sigma_x &= \Gamma - \Gamma F_s^T(\lambda I + F_s\Gamma F_s^T)^{-1}\Theta\Gamma \\ \mu_x &= \Gamma F_s^T(\lambda I + F_s\Gamma F_s^T)^{-1}y_M, \end{aligned} \tag{15}$$

and $\Gamma = diag(\gamma_i)$. The task is to determine each γ_i, which is equivalent to conduct

$$\begin{aligned} \gamma &= \arg\min_\gamma \int \mathbf{p}(y_M|x)\,|\mathbf{p}(x) - \mathbf{p}_\gamma(x)|\,dx \\ &= \arg\max_\gamma \int \mathbf{p}(y_M|x)\prod_i \mathcal{N}(x_i;0,\gamma_i)\varphi(\gamma_i)dx_i. \end{aligned} \tag{16}$$

This results in the well-known SBL cost function under improper prior $\propto 1/|x_i|$

$$\mathcal{L}_{\text{SBL}} = \log|\Sigma_{y_M}| + y_M^T\Sigma_{y_M}^{-1}y_M, \tag{17}$$

where $\Sigma_{y_M} = \lambda I + F_s\Gamma F_s^T$. Both (12) and (17) can lead to sparse solution, i.e. the sparsity of $\hat{x}$ has $K = \|\hat{x}\|_0 \leq n$. Furthermore, the corresponding the squared error, i.e. $e = \|x - \hat{x}\|_2^2$, can be given as

$$e = \|x_\Lambda - \hat{x}_\Lambda\|_2^2 = \|x_\Lambda - Cx_\Lambda - D\epsilon_M\|_2^2 \tag{18}$$

where Λ denotes the set union of the positions of the non-zero elements in x and $\hat{x}$ (let $\Psi = F_{s,\Lambda}$ is a square matrix in worst case.), and $C = (\Psi^T\Psi + \lambda I)^{-1}\Psi^T\Psi$ and $D = (\Psi^T\Psi + \lambda I)^{-1}\Psi^T$. Then, (18) can be given as

$$\begin{aligned} e =& x_\Lambda^T x_\Lambda - 2x_\Lambda^T V S^2 (S^2 + \lambda I)^{-1} V^T x_\Lambda \\ &+ x_\Lambda^T V S^2 (S^2 + \lambda I)^{-2} S^2 V^T x_\Lambda \\ &+ x_\Lambda^T V^T \left[S^2(S^2+\lambda I)^{-2} S - (S^2+\lambda I)^{-1} S\right] U^T \epsilon_M \\ &+ \epsilon_M^T U \left[S(S^2+\lambda I)^{-2} S^2 - S(S^2+\lambda I)^{-1}\right] V^T x_\Lambda \\ &+ \epsilon_M^T U S (S^2+\lambda I)^{-2} S U^T \epsilon_M. \end{aligned} \quad (19)$$

Obviously, e is strongly depending on the choice of λ, which is usually difficult to obtain especially for an ill-conditioned Ψ. A lot of previous work have been investigated to estimate a proper λ. Let's consider the ultra sub-optimal case, i.e. $\lambda \to 0$, then (19) becomes as

$$\begin{aligned} e \to \epsilon_M^T U S^{-2} U^T \epsilon_M &= \left\| S^{-1} U^T \epsilon_M \right\|_2^2 \\ &\le \left\| S^{-1} \right\|_2^2 \left\| \epsilon_M \right\|_2^2 = \frac{\left\| \epsilon_M \right\|_2^2}{\min\{s_i^2\}}. \end{aligned} \quad (20)$$

In this work, we propose the noise mitigated method to reduce the error in (20) for a stable solution, wherein we have to modify the problem in (12) as

$$\min \left\| \Theta x - y_M \right\|_2^2 + \lambda \left\| x \right\|_p^p, \quad p \in [0, 1] \quad (21)$$

where $\Theta = [F_s, E]$ and E is an extended matrix (it can be a random matrix). The great advantage of this method is that e is less dependent on the choice of λ. A generalized solution is then

$$\hat{x} = [\hat{x}_{F_s}; \hat{x}_E] = \Gamma\Theta^T(\lambda I + \Theta\Gamma\Theta^T)^{-1} y_M. \quad (22)$$

More details can be found in [2] and the corresponding error upper bound can be given as

$$\begin{aligned} \left\| \hat{x}_{F_s} - x \right\|_2 \le& \kappa \cdot \frac{\sqrt{1+\delta_{2K}^{\Theta}}}{1-\delta_{2K}^{\Theta}} \left(\left\| \epsilon_M \right\|_2 + \frac{\sigma_K(x)_1}{\sqrt{K}} \right) \\ \ll& \frac{\sqrt{1+\delta_{2K}^{F_s}}}{1-\delta_{2K}^{F_s}} \left(\left\| \epsilon_M \right\|_2 + \frac{\sigma_K(x)_1}{\sqrt{K}} \right), \end{aligned} \quad (23)$$

if F_s is ill-conditioned and E is an orthogonal matrix. Furthermore, δ_{2K}^{Θ} and $\delta_{2K}^{F_s}$ are the $2K$-order restricted isometric property (RIP) constants of Θ and F_s, $\kappa \in (0, 1]$ is the mitigation factor, and $\sigma_K(x)_1$ is the best l_1-norm approximation error. That is

$$\sigma_K(x)_1 = \inf_{\|v\|_0 \le K} \left\| x - v \right\|_1. \quad (24)$$

4. SIMULATION AND APPLICATION

To validate the EBPSM and the processing de-noising algorithm. We build a 2D inhomogeneous medium model with two layer and 4 buried objects as figure (3a). The radar system is located on the $z = 0$. By simulation, the reflection signal from inhomogeneous medium is obtained. The reflection signal image with 15 dB signal to noise ratio (SNR) in time domain is as figure (3b). By using EBPSM and EBPSM with de-noising, the reconstructed radar images are separately as figure (3c) and figure (3d). The entropy value of signal image, EBPSM processed image and EBPSM with de-nosing processed image are 4.52, 3.96 and 2.52 separately.

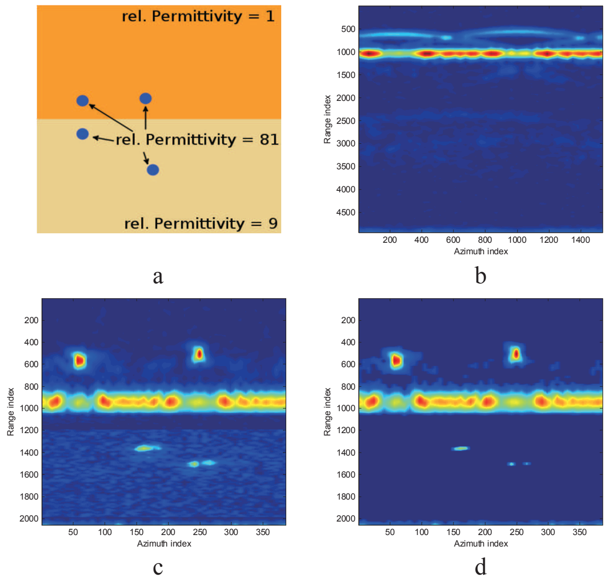

Figure 3: Effects of the de-noising on the performance of EBPSM. a) Simulation setup. b) Radargram. c) EBPSM. d) EBPSM + De-Noising.

Obviously, the processed image by EBPSM with de-noising is better than it by EBPSM. Additionally, the EBPSM with de-noising has been applied to the imaging of human body lumbar vertebrae yielding good results from data obtained in an anechoic chamber.

5. CONCLUSIONS

In this paper we introduced and analysed the EBPSM algorithm with de-nosing applied to human body area radar imaging. Simulation results demonstrate the superiority of EBPSM+De-Noising over conventional algorithms by means of imaging quality detection rate and false alarm rate. The EBPSM+De-Noising also works well for high permittivity scatterers in inhomogeneous media. EBPSM has been successfully applied to the imaging of human body lumbar vertebrae. In further steps the algorithms will be extended for more complex media and applied to a real time measurement system of the human spine.

6. REFERENCES

[1] G. W. K. Gu and J. Li. Migration based sar imaging for ground penetrating radar systems. *IEE Proc.-Radar Sonar Navig*, 151(5):1–9, Oct. 2004.

[2] Y. Lu, C. Scheunert, E. Jorswieck, and D. Plettemeier. Noise mitigated compressed sensing. *37-th International conference on telecommunications and signal processing*, 0(0):1–4, June 2014.

[3] H. Zhang, W.-S. Benedix, D. Plettemeier, and V. Ciarletti. Radar subsurface imaging by phase shift migration algorithm. *EuRAD*, 0(0):1–4, Oct. 2013.

[4] H. Zhang and D. Plettemeier. Subsurface imaging method (ssim) based on phase compensation of radar echoes. *EuCAP.*, 0(0):1–4, April 2010.